Article type: Original

The role of track stiffness and its spatial variability on long-term track quality deterioration

I. Grossoni[1*], A. R. Andrade[2], Y. Bezin[1], S. Neves[1]

[1] University of Huddersfield, Huddersfield, UK

[2] IDMEC, Instituto Superior Técnico, University of Lisbon, Lisboa, Portugal

Abstract

With rapid advances in sensor and condition monitoring technologies, railways infrastructure managers are turning their attention towards the promises that digital information and big data will help them understand and manage their assets more efficiently. In addition to existing track geometry records, it is evident that track stiffness is a key physical quantity to help assess track quality and its long-term deterioration. The present paper analyses the role of the track stiffness and its spatial variability through a set of computational experiments, varying other vehicle and track physical quantities such as vehicle unsprung mass, speed and track vertical irregularities. The support stiffness conditions are obtained using a sample procedure from an Autoregressive Integrated Moving Average (ARIMA) model to generate representative larger set of data from previously on-site measured data. A set of computational experiments is carefully designed, varying different physical variables, and a vehicle-track interaction model is used to estimate track geometry deterioration rates. A series of log-linear regression models are then used to analyse the impact of the tested physical variables on the track deterioration. The main findings suggest that the spatial variability of track stiffness contributes significantly to the track deterioration rates, and thus it should be used in the future to better target design and maintenance of railway track. Finally, a comparative study of some settlement models available in literature shows that they are very dependent on the test conditions under which they have been derived.

Keywords

Vehicle-track interaction, track stiffness, spatial variability, ARIMA, track quality, settlement, ballast, track irregularity, horizontal level.

1. Introduction

[*] Corresponding author: Ilaria Grossoni, University of Huddersfield, Queensgate, Huddersfield, HD1 3DH, West Yorkshire, UK. Email: i.grossoni@hud.ac.uk

Usually, track stiffness is the measure used to describe the quality of the support conditions and the track stability [1]. It is defined as the ratio of the load applied to the rail over the vertical rail deflection [2]. Ideally, this parameter is constant over a track section, but in reality this condition is very unlikely to happen. Some reasons are the non-uniformly compacted ballast layer, some local drainage problems as non-effective sub-ballast layer, non-uniformity in the subgrade properties or the presence of voids between sleeper / ballast interface. This non-uniformity in support stiffness, coupled with the permanent strain level (embedded geometry), produces a non-uniformity in track loading and track deterioration (differential settlement) that lead to track quality deterioration, driving up maintenance needs and costs.

Despite the major role played by track stiffness in the system long-term behaviour, it is very difficult to derive a measure of the actual variability of the track stiffness along the railway, most and foremost because the global stiffness is a combination of stiffness reaction from the various layers making up the railway track. It is therefore difficult to measure it with non-intrusive techniques. However, there are many experimental techniques which have been developed to acquire those values, for example using the Falling Weight Deflectometer (FWD) equipment or the Swedish Rolling Stiffness Measurement Vehicle (RSDV) measuring train [3], to name just a couple amongst a large number reported in previous research projects (Innotrack [4] and Rivas [5]). In the first case, FWD is an intrusive technique that requires track possession and estimates directly the stiffness of the support underlying the sleeper. In the latter, the RSDV measurements are taken from on-board a vehicle at a given speed and at rail level, therefore including the rail-pad layer and rail bending stiffness. In the first case, the FWD methodology is usually rather costly to deploy and the data acquired may not be long enough to be statistically representative of a site of interest. In the second case, while distance covered by the RSDV continuous measurement present a significant advantage, it still poses a problem to back filter and estimate the actual support stiffness below the superstructure (Winkler approximation). Nevertheless, it is important to note that the lack of reliable and long data makes it very difficult at present to derive a clear correlation between the physical properties of the railway system and its long-term behaviour.

In the past, several authors investigated the role of spatially varying track stiffness on both the contact forces and the track deterioration (e.g. [6-10]). Nevertheless, it seems there is a gap in the literature regarding a mathematical relationship between these two variables, and therefore, the main aim of the present study is to assess the role of spatial variability of the vertical track stiffness on the long-term behaviour of the track degradation. To achieve that, the present paper put forward a sample procedure to generate vertical stiffness signals that are representative from what can be found or measured in a railway track, i.e. that have similar statistical properties, namely the spatial variability of these vertical stiffness signals. Moreover, vertical track irregularities are also simulated, given a finite set of measured values. Both signals, i.e. vertical stiffness and vertical irregularities, are then used as an input in a vehicle-track interaction model to predict track forces in the time domain and derive long-term settlement of the track using state-of-the-art settlement laws. The novelty of this approach resides in the way the spatial variability is controlled, using Autoregressive Integrated Moving Average models (ARIMA) to take into account the spatial correlations of the input data, and then simulate/generate naturally occurring variations. Furthermore, the use of log-linear

regression models to relate track settlement, track stiffness and track irregularities from the computational results of the vehicle-track interaction model is original. Finally, quantitative considerations about established settlement models are also discussed in detail.
The outline of the present paper is the following: section 2 puts forward the methodology followed in the paper. A comparison of the settlement laws previously considered in the VTI model is provided in section 3. Section 4 provides the analysis of the computational experiments to relate the ballast settlement rate with the support stiffness and the rail irregularity profiles, using log-linear regression models on the computational results of the VTI model. Finally, section 5 explores the main conclusions, discusses the potential limitations and points new directions for future research.

2. Methodology

This methodology section starts with the aim and main assumptions made in subsection 2.1, and provides a statistical analysis and a simulation procedure for the support stiffness data (subsection 2.2) and for the vertical rail irregularities (subsection 2.3). Finally, details on the vehicle-track interaction (VTI) model are provided in subsection 2.4.

2.1. Aims and assumptions

The aims of this study are:

- to estimate a mathematical relationship between the track degradation and the variation in support stiffness,
- to assess the contribution of vehicle characteristics in the long-term track system behaviour.

The following assumptions have been made:

- The measured support stiffness and track vertical irregularity series have been modelled using Autoregressive Integrated Moving Average models (ARIMA) models, which are independent from each other;
- A vertical vehicle-track interaction model has been used including one bogie and two wheelsets;
- The long-term track behaviour has been predicted using the Guerin's settlement law which has been derived in laboratory for high speed lines;
- The unsprung mass and the travelling speed have been varied as vehicle characteristics. Further investigations have been made to assess the influence of axle load.

2.2. Support stiffness

The statistical analysis of the vertical support stiffness is divided into two parts: i) statistical distribution and ii) analysis of spatial correlations.

2.2.1. Statistical distribution of support stiffness

Two sets of sleeper support stiffness data have been analysed (sites A and B), whose main characteristics are reported in Table 1. The data was measured in the U.K. using the FWD equipment. Site A exhibits a mean value of 84.6 kN/mm and a range of almost 100

kN/mm, from a maximum value of 143.8 kN/mm to a minimum of 44.4 kN/mm; whereas site B exhibits a mean value of 110.4 kN/mm and a similar range of almost 100 kN/mm, from a minimum of 59.8 kN/mm to a maximum of 157.9 kN/mm.

Table 1: Main statistics of the measured sites.

	Number of measured sleepers	**Support stiffness mean value [kN/mm/ sleeper end]**	**Support stiffness standard deviation [kN/mm/ sleeper end]**	**Minimum value kN/mm/ sleeper end]**	**Maximum value kN/mm/ sleeper end]**	**K-S test p-value**
A	155	84.6	14.4 (σ^2 = 208)	44.4	143.8	0.32
B	80	110.4	16.2 (σ^2 = 262)	59.8	157.9	0.90

Normal probability distributions were fit to each dataset and are shown in Figure 1. The hypothesis that vertical support stiffness follows a normal distribution is not rejected at the 10% significance level [11], for site A (p=0.32) and for site B (p=0.90), according to the Kolmogorov-Smirnov (K-S) goodness-of-fit test (Table 1).

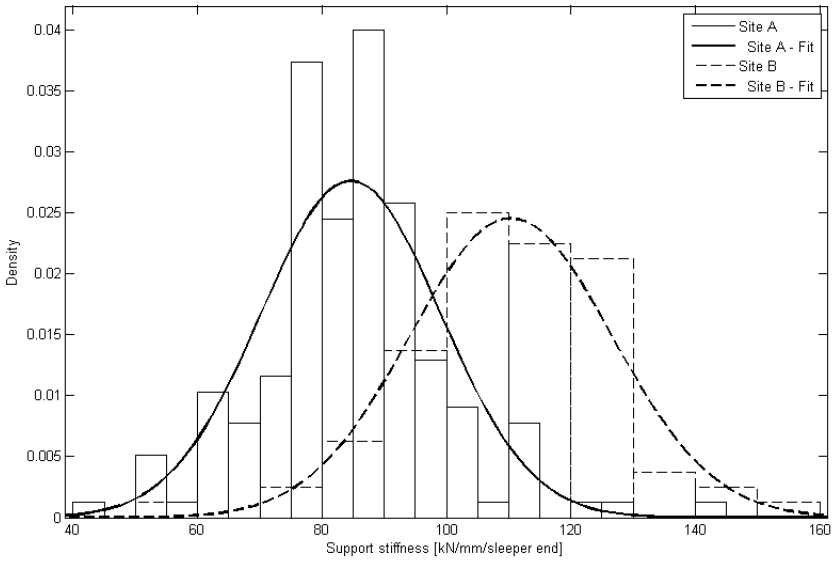

Figure 1: Histograms and normal distributions for the two sites A and B.

2.2.2. Analysis of spatial correlations of support stiffness

The normal probability distribution can then be used to generate any number of datasets with the same mean and standard deviation of sites A and B. However, such procedure would assume that each support stiffness would be independent from each other, which is not realistic. In fact, there is a continuity in support stiffness, i.e. there is a spatial correlation between consecutive values of support stiffness. Therefore, another kind of simulation procedure should be pursued in order to take into account the correct spatial

distribution of stiffness, i.e. the correct variation between one sleeper and the next one along the track.

In order to reproduce the spatial properties of the measured data, the ARIMA modelling approach has been used in the present study [12]. In a general way, the ARIMA model includes three components: a mean component (μ) and/or a weighted sum of neighbouring values ($W_{t-\mathrm{k}}$) and/or a weighted sum of neighbouring error values (e_t). This means that any data point uses values that precede it plus some random error in order to respect a certain continuity of the original signal.

From a mathematical point of view, a time series $\{Y_t\}$ is said to follow an ARIMA model if the dth difference $W_t = \nabla^d Y_t$ (i.e. the signal is replaced with dth difference of its values and the previous values) is a stationary Autoregressive Moving Average (ARMA) process. The AR part indicates that the variable is regressed on its own prior values, the MA part indicates that the regression error is actually a linear combination of error terms and the stationarity implies that the series remains at a fairly constant level over time. If $\{W_t\}$ follows an ARMA (p, q) model, then $\{Y_t\}$ is an ARIMA (p, d, q) process. For practical purposes, values for d are usually assumed to be equal to 1 or at most 2. For instance, for a stationary ARIMA (p, 0, q) model with d=0 and with a mean equal to μ:

$$W_t = \mu + \varphi_1 W_{t-1} + \varphi_2 W_{t-2} + \cdots + \varphi_p W_{t-p} + e_t - \theta_1 e_{t-1} - \theta_2 e_{t-2} - \cdots - \theta_q e_{t-q} \quad (1)$$

Different model specifications can be compared based on the Akaike's Information Criterion (AIC) [13]:

$$\mathrm{AIC} = -2\log(L^*) + 2k \quad (2)$$

Where L* is the maximum likelihood and k is the number of parameters (k=p+q+1). Other information criteria include the corrected AIC for ARIMA models (AICc):

$$\mathrm{AICc} = \mathrm{AIC} + \frac{2\cdot(p+q+k+1)\cdot(p+q+k+2)}{T-p-q-k-2} \quad (3)$$

And the Bayesian Information Criterion (BIC):

$$\mathrm{BIC} = \mathrm{AIC} + (\log T - 2)\cdot(\mathrm{p}+\mathrm{q}+\mathrm{k}+1) \quad (4)$$

All the criteria mentioned allow the selection of the best ARIMA model based on the one with minimum criterion value. Table 2 shows the best ARIMA model according to the AIC, AICc and BIC criteria for each site. Note that for site A, the ARIMA (5, 1, 0) model is consistently chosen according to the three criteria; though for site B, there is no consistent model for all the three criteria, i.e. the ARIMA (2, 1, 0) model with a drift term is chosen according to the AIC and AICc criteria whereas the ARIMA (1, 1, 1) model is chosen according to the BIC criterion.

Table 2: Best ARIMA model (in italics) according to the AIC, AICc and BIC criterion.

Site	**AIC**	**AICc**	**BIC**
A	*ARIMA (5, 1, 0)* AIC=1231.69	*ARIMA (5, 1, 0)* AICc=1232.26	*ARIMA (5, 1, 0)* BIC=1249.91
B	*ARIMA (2, 1, 0) with drift* AIC=664.94	*ARIMA (2, 1, 0) with drift* AICc=665.48	*ARIMA (1, 1, 1)* BIC=673.11

Table 3 provides the best ARIMA models with estimated values for the associated parameters, with the respective standard deviations in parenthesis. Note that in case of

site B the BIC criterion has been considered to avoid a non-stationary model, i.e. models with drifts, and thus an ARIMA(1, 1, 1) is presented.

Table 3: ARIMA models with estimated values for each site analysed.

Site	**Model**	φ_1	φ_2	φ_3	φ_4	φ_5	θ_1	σ_e^2
A	ARIMA (5, 1, 0)	-0.5683 (0.0809)	-0.4721 (0.0905)	-0.4753 (0.0908)	-0.3511 (0.0898)	-0.0438 (0.0838)	-	160
B	ARIMA (1, 1, 1)	0.2621 (0.1211)	-	-	-	-	-0.9524 (0.0407)	243

By construction, the simulated data set based on the best ARIMA model follows the same ARIMA model.

An example of simulated series from each ARIMA model with coefficients as in Table 3 is reproduced in Figure 2(a,b) and compared with the original/raw data (in bold lines). In order to validate it, the percentage difference in terms of support stiffness gradient between raw data and simulated data has been calculated and it has been seen that it is generally lower than 10%, with few cases up to 23%. Note that for site B, simulated and original series are shorter with 80 values/sleepers and for site A with 155 values/sleepers. Figure 3 shows 500 statistical realisations per each site based on the best ARIMA model found (see Table 3), including the 5th and the 95th percentile.

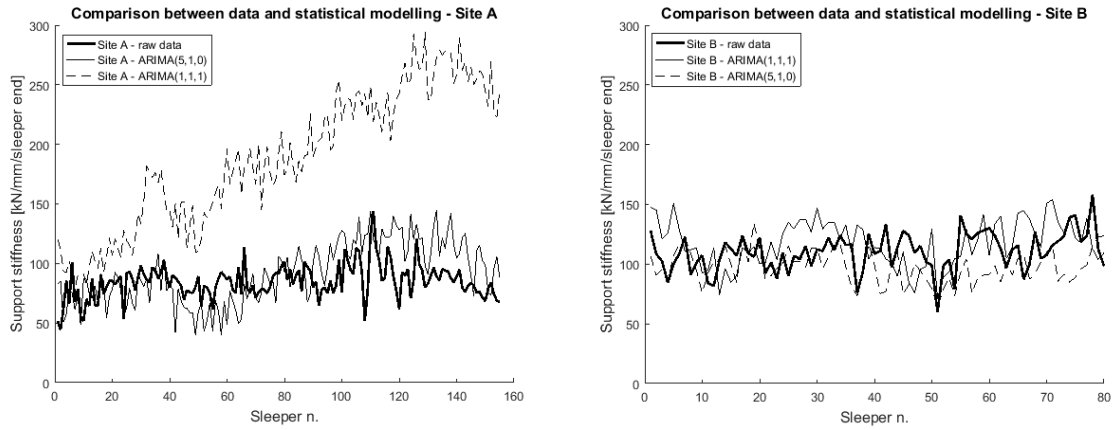

(a) (b)

Figure 2: (a,b) Comparison between the original data (bold lines) and the data simulated/obtained with the ARIMA statistical models.

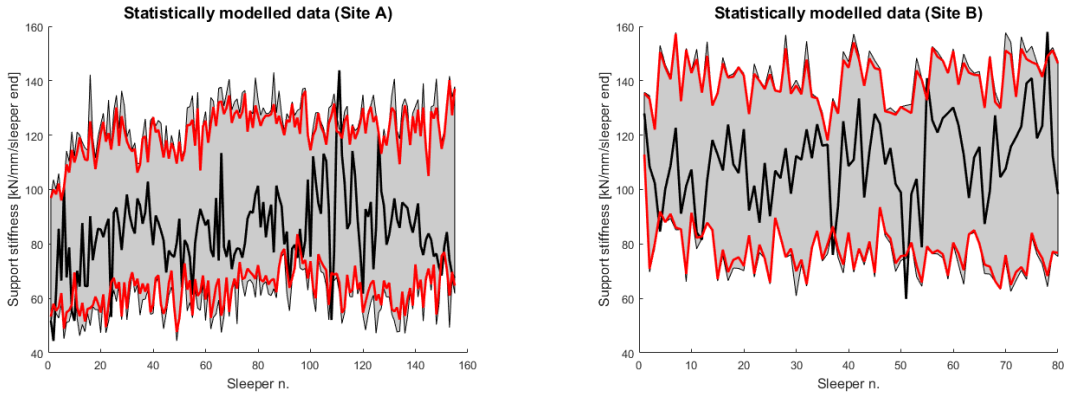

(a) (b)

Figure 3: 500 statistical realisations for (a) site A and (b) site B (black line: original data set; grey area: 500 statistically modelled realisations; red lines: 5th and 95th percentile).

From fitting ARIMA models to both sites, it is possible to conclude that there is no consistent ARIMA model for both sites analysed, i.e. no model specification (p, d, q) can describe the track stiffness regardless of the site. This might be because it is not possible to represent the localised characteristics in a general way, or might be due to the lack of long data series. For instance, for site A the ARIMA(5, 1, 0) model is considered the best ARIMA model, whereas for site B it is the ARIMA(1, 1, 1) model.

Regarding the advantage of using ARIMA models, it is worth noting that the variance of the error term σ_e^2 (not the total variance of the series) reduces in all cases, when the first order difference is controlled through the neighbour values. For example, for site A the uncontrolled variance of the support stiffness changes from a variance of 208 (Table 1) to 160 (Table 3), representing a reduction of the variance of the error term of around 23%. For site B, the similar reduction is only 8%.

Moreover, the ARIMA modelling provides a way to reproduce a theoretically infinite number of series with a given mean value μ and a standard deviation σ by taking advantage of a property of ARIMA stochastic processes, according to which a linear transformation of an ARIMA stochastic process is also an ARIMA stochastic process:

$$w_t = \alpha . W_t + \beta \quad (5)$$

Where w_t is the new series, W_t the original series and α and β are selected constants so that the new series has a given mean m and standard deviation σ, i.e. $\alpha = \sigma/VAR[W_t]$ and $\beta = m - \alpha \cdot E[W_t]$, in which $E[W_t]$ and $VAR[W_t]$ are the mean and the variance of the original series.

Figure 3 provides a simulated series of length (n=100 values/sleepers) from the ARIMA(5,1,0) model (site A) with m=96.6 kN/mm and σ=22.3 kN/mm and four transformations, with mean ranging from m=60 kN/mm to m=80 kN/mm and standard deviation ranging from σ=5 kN/mm up to σ=10 kN/mm.

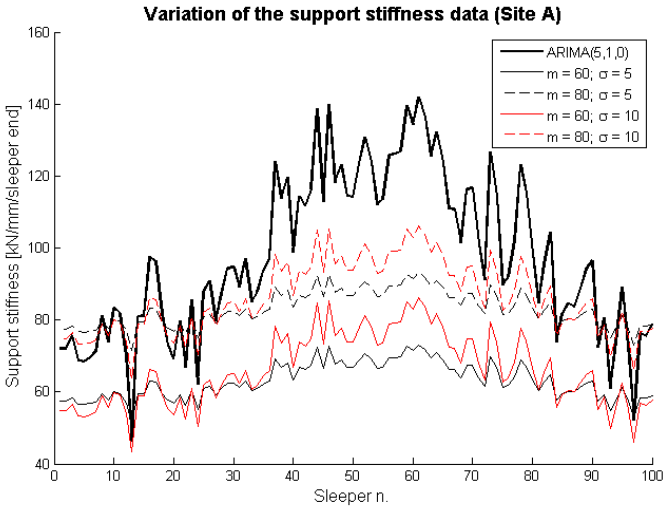

Figure 4: Variation of the best ARIMA model changing the mean value m and standard deviation σ (site A).

It should be mentioned that simulating from ARIMA models might fluctuate to very extreme values, as ARIMA models control for consecutive/neighbour values, and even very odd cases for this physical example may happen, i.e. we might simulate negative values at some points for the vertical stiffness. Thus, it is common to limit these extreme values (minimum and maximum) by simulating several sets of data and only use those that have all values lower than the maximum and higher than the minimum. In addition, for a given ARIMA model, it is possible to generate a theoretically infinitely long new series. This characteristic has been used in the following analysis simulating a 200-metre long track (i.e. a track section).

2.3. Vertical rail irregularities

Statistical modelling of the vertical rail irregularities, i.e. the top level series filtered between 2 and 25 meters, focuses in the analysis of spatial correlation and the potential co-integration of this series with the previous series of support stiffness.

2.3.1. Analysis of spatial correlations of vertical rail irregularities

Another input that needs to be statistically modelled, so that one can sample from that model, is the vertical irregularities. The vertical irregularities have been measured with the Track Recording Coach at the same time of the support stiffness measurements. Track geometry records have been sampled every 0.269 m.

Similar to the case of support stiffness, the vertical rail irregularities have also been statistically modelled using ARIMA models, namely with the use of "Simulate.Arima" function from "Forecast" package in R [14]. Moreover, the two data sets from each site (A and B) were analysed and the best ARIMA model was estimated according to the AIC, AICc and BIC criterion, finding that the ARIMA(5, 0, 0) model was consistently selected as the best model according to any of the three criteria for site A, and that the ARIMA (3, 0, 2) model with non-zero mean was selected as the best model according to

the AIC and AICc criteria and the ARIMA (3, 0, 2) model was selected as the best model according to the BIC criterion.

Table 4: Best ARIMA model (in italics) according to the AIC, AICc and BIC criterion.

Site	AIC	AICc	BIC
A	*ARIMA (5,0,0)* AIC=-345001.4	*ARIMA (5,0,0)* AICc=-345001.4	*ARIMA (5,0,0)* BIC=-344955.3
B	*ARIMA (3,0,2) with non-zero mean* AIC=-30817.78	*ARIMA (3,0,2) with non-zero mean* AICc=-30817.71	*ARIMA (3,0,2)* BIC=30785.05

Similar to the support stiffness case, it is important to mention that there is no agreement with the best ARIMA model for both sites.

Table 5 provides the estimated values for the associated parameters of the best ARIMA models for each site, with the respective standard deviations in parenthesis. Note that all estimates are statistically significant at the 10% significance level, based on a t-student test.

Table 5: ARIMA models with estimated values for each site analysed.

	Model	φ_1	φ_2	φ_3	φ_4	φ_5	θ_1	θ_2	σ_e^2
A	ARIMA (5, 0, 0)	4.3574 (0.0040)	-7.9951 (0.0144)	7.7622 (0.0208)	-3.9892 (0.0144)	0.8645 (0.0040)			$3x10^{-5}$
B	ARIMA (3,0,2)	2.6438 (0.0171)	-2.4077 (0.0337)	0.7619 (0.0171)			0.5784 (0.0230)	0.6076 (0.0189)	$3.8x10^{-4}$

Having estimated the ARIMA models for the vertical support stiffness and rail irregularities, one can discuss whether or not the datasets are correlated for each site, or whether or not the independence assumption can hold. To test that, subsection 2.3.2 explores the potential co-integration between the two series: support stiffness and vertical irregularities.

2.3.2. Correlation between support stiffness and rail irregularity

Two statistical tests are applied to explore the potential co-integration between the support stiffness and the vertical irregularities series. First of all, the independent random walk hypothesis (i.e. if the series contain unit roots) is discussed using the augmented Dickey-Fuller [15] and the Phillips-Perron [16] tests. If the p-values are higher than 5%, the null hypothesis that the series have unit roots at the 5% significance level is retained. The results are shown in Table 6.

Table 6: Testing the independent random walk hypothesis.

Series	Test	Site A			Site B		
		Result	***Lag order***	***p-value***	***Result***	***Lag order***	***p-value***
Support stiffness	Dickey-Fuller	-2.8378	5	0.2272	-3.025	4	0.1563

	Phillips-Perron	-11.1720	4	0.4736	-17.721	3	0.0917
Track irregularities	Dickey-Fuller	-3.3253	5	0.0696	-4.6952	4	**0.0100**
	Phillips-Perron	-88.2270	4	**0.0100**	-64.350	3	**0.0100**

From Table 6 it is possible to conclude that the non-stationary hypothesis is rejected in case of support stiffness for both sites and according to both tests. On the contrary, in the case of track irregularities signals, this hypothesis is rejected only for site A and according to the Dickey-Fuller test. This means that it is possible to apply the ARIMA modelling to the series considered.

The cointegration between the support stiffness and the track irregularities series is then assessed using the Phillips-Ouliaris cointegration test [17]. In both site cases, the null hypothesis is rejected, i.e. the two series are not co-integrated. Since there is no evidence of cointegration, the use of a multivariate ARIMA model is not justified and, then, it is assumed that both signals can be simulated independently from each other.

Finally, a further test has been carried out fitting a VAR model using the support stiffness and the track irregularities series for each site considered. It has been seen that each series has statistically significant predictors only from the series itself, which is in line with no evidence of co-integration for both series. However, there could be some correlation expected if longer datasets were studied and additional wavelength measurements. This is out of scope of the present work, and as no additional data is available at this time, this idea is left for further research.

2.4. Vehicle-track interaction model and long-term behaviour

The model used in the present study to calculate the vehicle-track interaction is shown in Figure 5 and consists in a beam on discrete support for the track and multibody system for a quarter vehicle model.

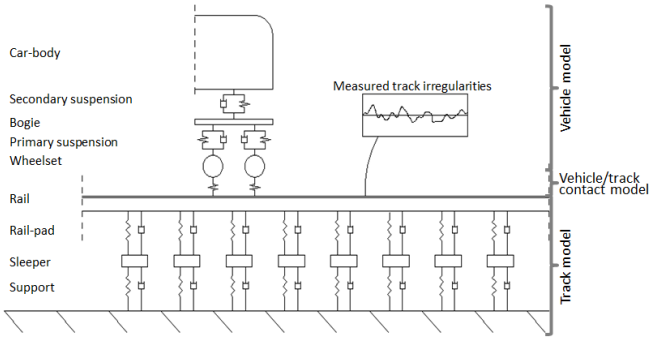

Figure 5: Vertical vehicle-track interaction model.

2.4.1. Finite element track model

The rail is modelled as a Timoshenko beam. A finite element approach is developed approximating the deformation of the rail within an element using nodal values of

displacement and rotation and assuming a third order Hermitian interpolation. Four beam elements are considered within each sleeper-spacing considered sufficient to achieve a good resolution of results [18].
The beam is characterized by the mass per unit length $\bar{m}_r$, the steel density ρ, the cross-sectional area A, the element length l, flexural rigidity EI, the shear coefficient κ and the shear modulus G. The sleepers are represented by their effective mass m_s, and assumed to be concentrated in the centre of gravity. The support is represented by rail-pad and the sleeper-ballast interface. The rail-pad layer is characterized by a linear spring of stiffness k_r in parallel with a damper having viscous damping coefficient c_r, the sleeper-ballast layer similarly by a linear spring of stiffness k_b and a damper in parallel with constant c_b.
The main track parameters used in the model are:

- *Rail section*: 60E1;
- *Rail pad vertical dynamic stiffness*: 270 MN/m (medium-hard rail pad);
- *Vertical support stiffness*: as calculated in the previous paragraph;
- *Rail vertical irregularities*: as calculated in the previous paragraph;
- *Sleeper mass*: 308 kg (typical concrete sleeper);
- *Sleeper spacing*: 0.65 m.

2.4.2. Vehicle multibody system model

The model used here consists of a quarter car supported by a bogie through the secondary suspension and a bogie supported by two half wheelsets through the primary suspension. All the bodies are assumed to be rigid. The car body is represented by its mass M_c, the bogie by its mass M_t and its pitch moment of inertia J_t and the wheelset by its mass M_w. Each primary suspension is modelled as a spring of stiffness K_{s1} in parallel with a damper with viscous constant C_{s1}. Similarly, the secondary suspension is characterized by a linear spring of stiffness K_{s2} in parallel with a dashpot having viscous constant C_{s2}. These two sub-systems are coupled together through non-linear Hertzian contact [19].

2.4.3. Long-term system behaviour

The vertical model described is then used within an iterative process (Figure 6) to calculate the track long-term behaviour.

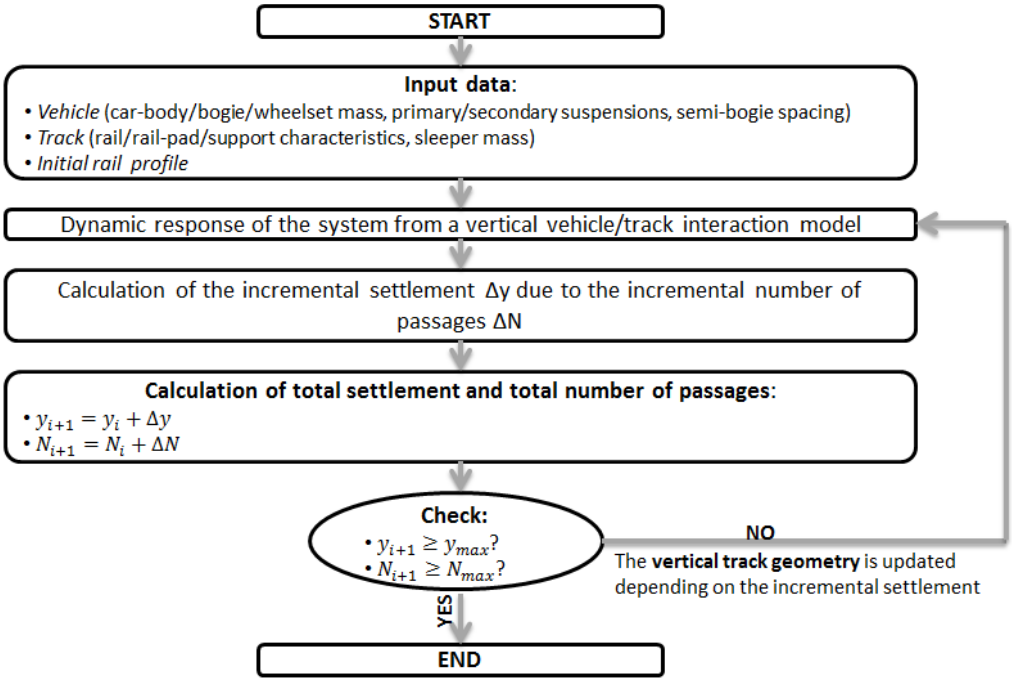

Figure 6: Flow chart of the iterative process used to calculate the track long-term behaviour.

In particular, after the initialization with the vehicle, track and vertical rail profile data, the dynamic response of the vehicle-track interaction system is calculated in terms of contact forces and displacements. The track settlement law is therefore applied and the incremental settlement Δy due to the incremental traffic ΔN is calculated. The total settlement is evaluated as the sum of the total settlement of previous iteration and the incremental settlement of the current one, as the plastic deformation is irrecoverable and the plastic deformations increase monotonically [20]. Finally, a check in terms of maximum settlement and maximum traffic is performed. In case it is not satisfied, the process continues updating the vertical track geometry depending on the incremental settlement.

3. Comparison of ballast degradation laws with potential application to the vehicle-track interaction model

There are a large number of settlement analytical models available in the literature, which have been empirically derived either from laboratory tests (i.e. tri-axial tests, reduced scale box test and full scale box tests) or *in situ* tests. A detailed critical review has been carried out in Dahlberg [21], considering Japanese (Sato models), US (Alva-Hurtado model, Ford model), European (ORE model, German models - Dietrich, Hettler, Holzlohner - , British – Shenton - , French– Guerin model), South African (Frohling), and Australian models.
The settlement values obtained from selected models have been compared in Figure 7, Figure 8 and Table 7 for up to 1M loading cycles.

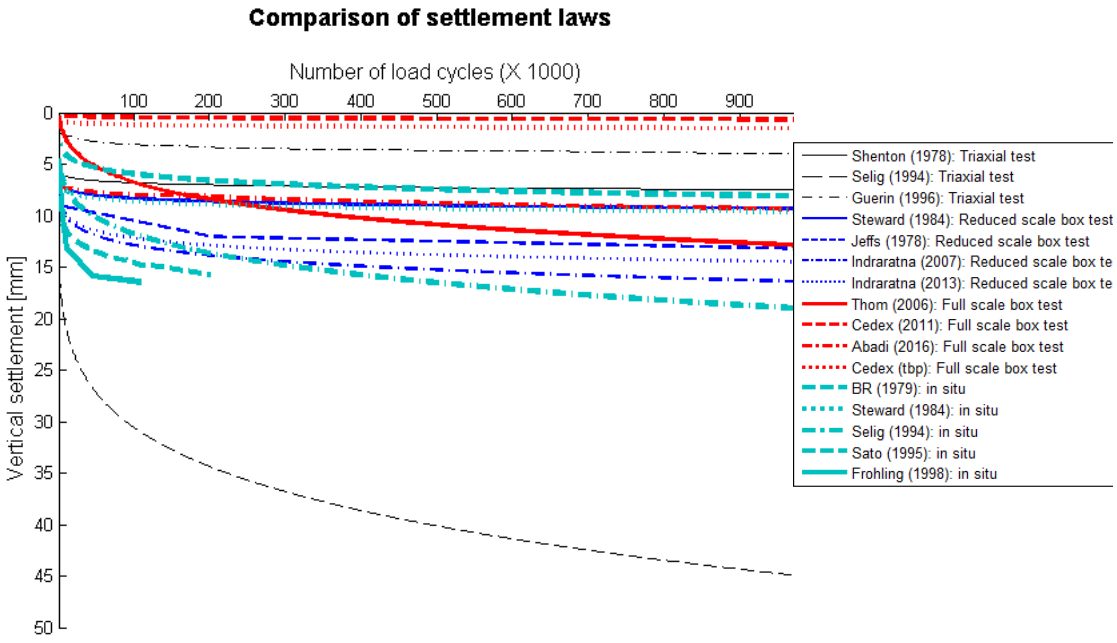

Figure 7: Comparison of settlement laws obtained from *in situ* (cyan lines), laboratory tri-axial (black lines), scaled box (blue lines) and full scale box (red lines) tests.

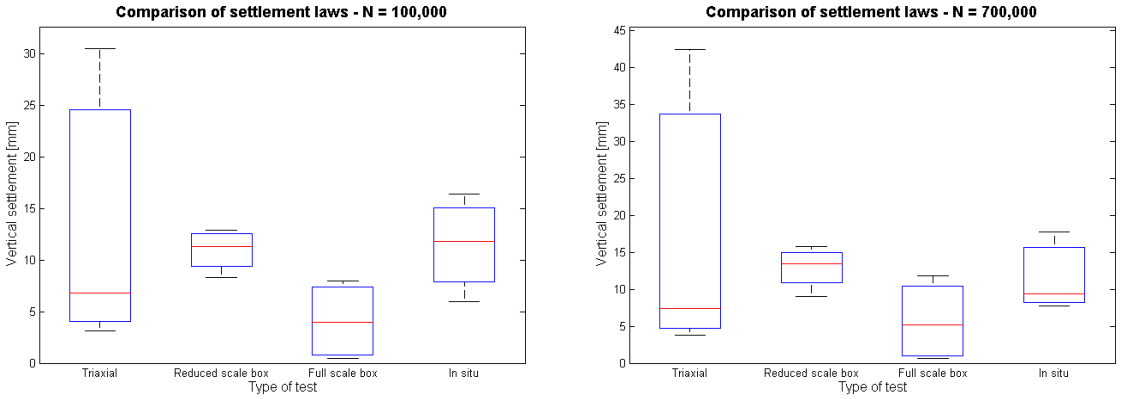

Figure 8: Comparison of settlement values obtained at 100,000 cycles (left plot) and 700,000 cycles (right plot).

Table 7: Settlement laws obtained with laboratory tests (S_N is the vertical settlement at the cycle number N and N' the number of passages per cycle).

Test type	**Author**	**Empirical law**	**Constants**
Triaxial test	Shenton [22]	$S_N = S_1 \cdot (1 + a \cdot \log_{10} N)$	a= 0.2
	Selig [23]	$S_N = g \cdot N^h$	g= 4.3; h= 0.17
	Guerin [24]	$dS_N/dN = i \cdot {d_{b,max}}^j$	i= 0.00000144; j= 2.51
Reduced	Steward	$S_N = S_1 \cdot (1 + m \cdot \ln N)$	m= 0.35 (0.63 if

scale ballast box test	[25]		uncompacted)
	Jeffs [26]	$S_N = \begin{cases} b + c \cdot \log_{10} N + d \cdot N, & N < 200000 \\ e + f \cdot N, & N \geq 200000 \end{cases}$	b= 90; c= 0.006; d= 0.00015; e= 12.5; f= 0.000015
	Indraratna [27-29]	$S_N = S_1 \cdot N^l$ $S_N = S_1 \cdot (1 + n \cdot \ln N + 0.5 \cdot o \cdot \ln N^2)$	k= 0.106 n= 0.43; o= 1.6
Full scale ballast box test	Thom [30]	$S_N = (\log_{10} N - 2.4)^2$	
	Cedex† [31, 32]	$S_N = p \cdot N^q$ $S_N = r \cdot N^s$	p= 0.07; q= 0.1625 r= 0.85; s= 0.18
	Abadi [33]		
In situ test	Partington [34]	$S_N = b \cdot (\log_{10} N)^c$	b= 0.29 (0.38 if high load); c= 1.77 (1.71 if high load)
	Steward [25]	$S_N = S_1 \cdot (1 + a \cdot \log_{10} N)$	a= 0.29
	Selig [23]	$S_N = g \cdot N^h$	g= 0.0035; h= 0.21
	Sato [35]	$S_N = i \cdot T^l \cdot V^j \cdot {M_s}^k \cdot L^m \cdot P^n \cdot N'$	i= 0.00209; l= 0.31; j= 0.98; k= 1.1; m= 0.21; n= 0.26
	Frohling [36]	$S_N = \left[o + p \cdot \left(\frac{K_s}{q}\right) \cdot \left(\frac{P_{dyn}}{P_{sta}}\right)\right]^{0.3} \cdot \ln N$	o= 194; p= -1.96; q= 1.34

Figure 7 and Figure 8 highlight the fact that, even though there is a large number of settlement laws available in the literature, it is still very difficult to find an agreement between the test conditions under which they have been derived and, therefore, between the results. Another fact is that it is very difficult to translate the laboratory conditions of triaxle tests to real track condition (i.e. definition of the confining pressure). Thus, a common test specification that takes into account the vehicle-track interaction point of view should be developed to harmonise the settlement laws.

Moreover, as pointed out in Dahlberg [21] (Table 7), most of the empirical laws show a dependency only on the number of cycles, and not on the actual dynamic conditions, such as vehicle speed and track conditions. This means that it is meaningless to use them in a vehicle-track interaction program. Two exceptions are Guerin law and Sato law.

Hereafter, a comparison is shown for different support conditions and different traffic type.

Three support stiffness and three types of traffic are compared (Table 8).

Table 8: Freight traffic and passenger traffic characteristics.

Parameter	**Freight traffic**	**Passenger traffic 1**	**Passenger traffic 2**

† The first settlement law has been derived using bituminous mix subballast sections.

		(regional multiple units)	**(intercity double decker)**
Axle load [t]	25	12	17
Speed [km/h]	80 (30)	150 (45)	250 (75)
Primary suspension stiffness [MN/m]	5	2	11
Support stiffness [kN/mm]	40 (soft track bed),80 (typical track bed),200 (stiff track bed) according to EUROBALT guidelines [37]		

The comparison of the settlement laws in case of the three levels of support stiffness and the three traffic types considered is presented in Figure 9.

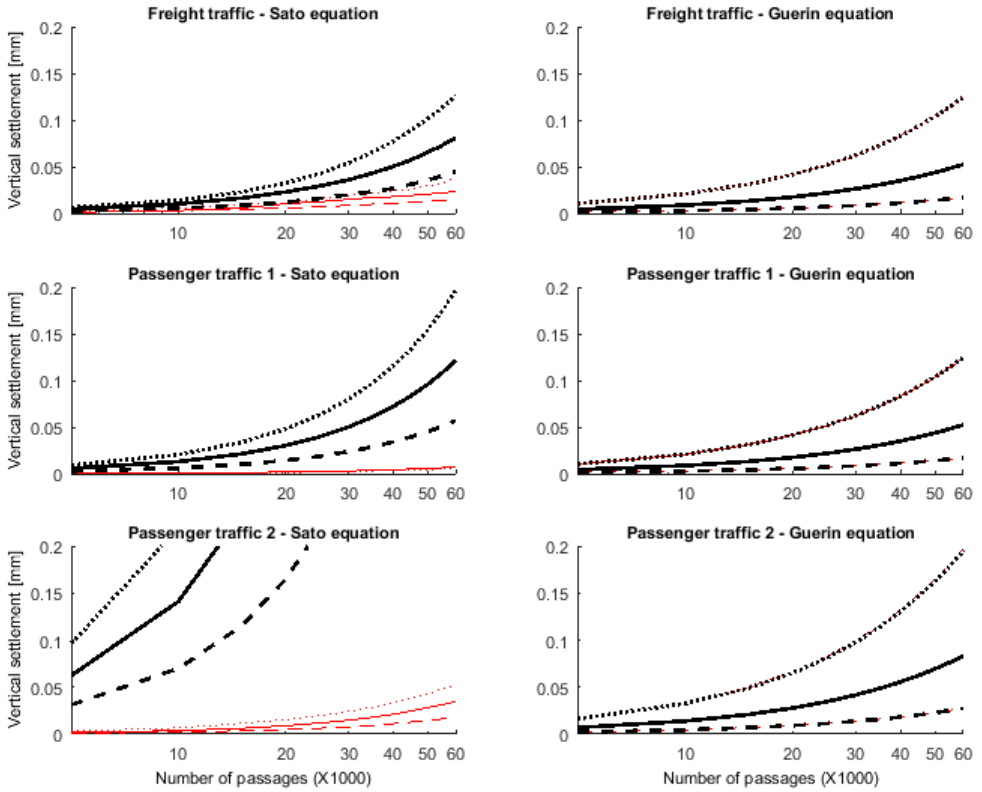

Figure 9: Comparison between settlement laws in case of three support stiffness and the three traffic types (black lines: maximum speed; red lines: reduced speed; dotted lines: soft track bed; continuous lines: typical track bed; dashed lines: stiff track bed).

From Figure 9 it is possible to conclude that the Sato law is very sensitive to the increase in speed, while the settlement calculated according to Guerin law is hardly affected. This can be explained with the fact that the first one has been derived starting from site measurements under very heavy freight traffic, while the second using tri-axial tests on ballast considering high speed lines. Ideally, a model tuned in between the two would be preferable, but this is not possible to judge at this time based on existing data and the choice is made to use Guerin and thus, to offer a conservative view.

Note that the proportion between the plastic element settlement and the resilient movement at each cycle is supported by the field experience, according to which the plastic settlement and elastic stiffness are related [38].

4. Analysis of computational experiments

This section explores and analyses the computational experiments that followed during this study. Subsection 4.1 provides an orthogonal design of experiments, subsection 4.2 explores the results and uses log-linear regression models to estimate the contribution of each variable, and finally subsection 4.3 focuses on the influence of speed and the axle load.

4.1. Design of experiments

The parameters considered in this study and their variations are reported in Table 9. Five variables are analysed: the mean ($\mu_{K,z}$) and the standard deviation ($\sigma_{K,z}$) of the vertical support stiffness, and the standard deviation of the rail irregularities (σ_Z), and the speed and the vehicle unsprung mass.

Table 9: Design of experiments.

Parameter	**Designation**	**Values**	**Unit**
Speed	S	40/80/120/160	km/h
Vehicle unsprung mass	USM	500/1000/1500	kg
Support stiffness mean value	$\mu_{K,z}$	60/80/100/120/140/160	kN/mm/sleeper end
Support stiffness standard deviation	$\sigma_{K,z}$	5/10/15/20	kN/mm/sleeper end
Rail irregularity standard deviation	SD	2.2/2.4/2.6/2.8/3.0/3.2/3.4/3.6/3.8/4.0	mm

Due to the high number of simulations planned, the High Performance Computing (HPC) facilities available at the University of Huddersfield have been used through the Condor platform [39]. A reduced design of experiments was pursued and a total of 1574 valid simulations were analysed.

4.2. Results

In order to provide a better understanding of the post-processing of the results of the computational experiments, a short example of the evolution of track irregularities is provided in Figure 10, which considers the Guerin settlement model.

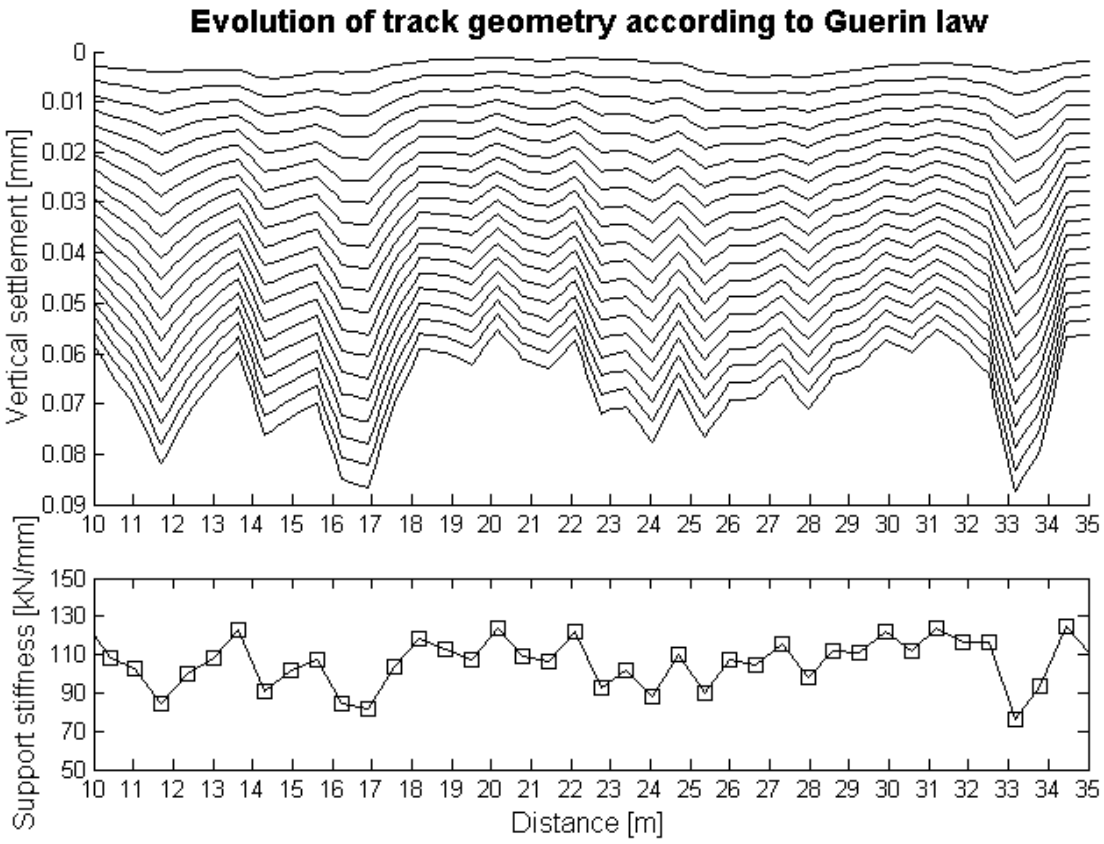

Figure 10: Example of evolution of track geometry due to non-uniform track considering Guerin's settlement model.

As expected, Figure 10 reveals that the support stiffness plays a fundamental role in the rail geometry degradation. High support stiffness leads to lower settlement than low support stiffness, and reciprocally soft spots tend to develop a localised dip in geometry (e.g. around 17 m or 33 m). This is in line with the findings from the EUROBALT project [37], according to which low track bed stiffness produces an increase in ballast settlement. Steenbergen [40] shows the strong correlation between transitions in dynamic stiffness and the initiation and rapid growth of ballast degradation. More recently, Nielsen et al. [41] based their research on 17 years of track geometry and support stiffness records along a heavy haul line and highlight that isolated defects often occur on track section with a combination of low magnitude and high gradient of support stiffness. Note that in each of the following calculations a track section of 200 m is considered, which is the typical length used by railway administrators to measure and quantify track quality.

Two dependent variables have been investigated: i) the deterioration rate of the ballast layer settlement SD (β_{SD_b}) and ii) the deterioration rate of the maximum ballast layer settlement (β_{max_b}). These two dependent variables were computed based on the evolution of the settlement of the ballast with accumulated tonnage. For example, in case of deterioration rate of the ballast settlement SD β_{SD_b}, firstly the standard deviation of

the signal along the track per each set of accumulated passage (ΔN) is calculated. The slope of the linear regression, thus, provides the deterioration rate.
A similar methodology is adopted to calculate the deterioration rate of the maximum ballast settlement β_{max_b}, taking the maximum value of the absolute signal per each accumulated passage.
The following step consists in relating both the degradation rates with the physical/explaining variables that were varied in the design of experiments. These are the mean of the vertical stiffness (μ_{K_z}), the standard deviation of the vertical stiffness (σ_{K_z}), the travelling speed (S), the unsprung mass (M_u) and the standard deviation of the vertical rail irregularities (SD). Main statistics of dependent and independent variables are presented in Table 10.

Table 10: Main statistics of the dependent and independent variables.

Variables			**Main statistics**			
			Mean	**SD**	**Min**	**Max**
Dependent	β_{SD_b}	mm/100 MGT	0.0741	0.0522	0.0111	0.2333
	$\beta_{\max\_b}$	mm/100 MGT	0.9899	0.5273	0.4773	2.7932
Independent	S	km/h	57.36	19.89	40	80
	M_U	kg	937.11	392.74	500	1500
	μ_{K_z}	kN/mm	110.69	34.55	40	160
	σ_{K_z}	kN/mm	14.28	7.35	5	30
	SD	mm	3.10	0.57	2.20	4.00

Log-linear regression models were estimated to assess the contribution of each independent variable in the variability of the dependent variables, with the following expressions:

$$\beta_{SD\_b} = \exp\left(\lambda_0 + \lambda_1.\mu_{K_z} + \lambda_2.\sigma_{K_z} + \lambda_3.M_U + \lambda_4.S + \lambda_5.SD\right) \quad (6)$$

$$\beta_{\max\_b} = \exp\left(\lambda_0 + \lambda_1.\mu_{K_z} + \lambda_2.\sigma_{K_z} + \lambda_3.M_U + \lambda_4.S + \lambda_5.SD\right) \quad (7)$$

Five models are explored, adding the independent variables sequentially, and selecting at each step the independent variable that most improves the coefficient of determination (R^2). For the first dependent variable (β_{SD_b}), model M1a uses only the mean of the vertical stiffness, model M2a adds the standard deviation of the vertical stiffness, model M3a adds the unsprung mass, model M4a adds the speed and finally model M5a adds the standard deviation of the vertical irregularities as independent/explaining variables. A similar procedure has been followed for the second dependent variable ($\beta_{\max\_b}$). All estimated models include an intercept parameter (λ_0). Table 11 provides the estimated log-linear regression models, with the estimated coefficients associated with each independent variable ($\hat{\lambda}_i$), the p-value relative to t-test and the coefficient of determination (R^2) for each model. Table 12 summaries the main key drivers for the dependent variables β_{SD_b} and β_{max_b}.
First of all, it should be pointed out that the mean of the vertical stiffness (μ_{K_z}), which is perceived as a strong indicator for track quality, is the independent variable that explains a higher portion of the linear variability of each dependent variable, with associated coefficients of determination of R^2=0.6506 and R^2=0.9304, for β_{SD_b} and $\beta_{\max\_b}$

respectively in models M1a and M1b. Note that this finding is in line with the state of the art, and the current focus that has been given to the vertical track stiffness as the main parameter in track quality assessment.
Some conclusions can be drawn as follows:

- Deterioration rate of the ballast settlement SD (β_{SD_b}):

the standard deviation of the vertical stiffness contributes to explain an additional portion of 26.4% (ΔR^2=0.9147-0.6506=0.2641) from the linear variability of β_{SD_b}. The inclusion of the unsprung mass in model M3a contributes to explain an additional portion of 0.8% (ΔR^2=0.9227-0.9147=0.0080), whereas the speed and the standard deviation of the vertical irregularities do not exhibit statistically significant coefficients (p=0.862 and p=0.904, respectively), and they do not contribute to improve the coefficient of determination. Note that the Guerin model assumed a low impact of vehicle speed (Section 3). Using the Sato model would have shown a big influence.

- Deterioration rate of the maximum defect of the ballast layer (β_{max_b}):

the inclusion of the unsprung mass in model M2b contributes to explain an additional portion of 0.37% (ΔR^2=0.9341-0.9448=0.0037) from the linear variability of β_{max_b}. The inclusion of the standard deviation of the vertical stiffness in model M3b contributes to explain an additional portion of 1.07% (ΔR^2=0.9448-0.9341=0.0107), whereas the inclusion of the speed in model M4b contributes to explain an additional portion of 0.07% (ΔR^2=0.9455-0.9448=0.0007) and the standard deviation of the vertical irregularities does not exhibit a statistically significant coefficient (p=0.958), and it does not contribute to improve the coefficient of determination.

Table 11 also shows that in model M3a, for the same unsprung mass and mean of the vertical stiffness, an increase of 10 kN/mm in the standard deviation of the vertical stiffness corresponds to a relative increase in the deterioration rates of 53.5% ($\hat{\lambda}_2 \times 10 = 0.535$) for the β_{SD_b}. This is line with previous findings in other set of simulations (Grossoni et al. 2015), though this time the speed is lower and might have inflated the influence of the vertical stiffness standard deviation.

Table 11: Estimated log-linear regression models.

Dependent variable	**Model**	**Independent variables**	$\hat{\lambda}_i$	**p-value**	$\mathbf{R^2}$
β_{SD_b}	M1a	(intercept)	-5.5239	< 0.0001	0.6506
		μ_{K_z}	-0.0176	< 0.0001	
	M2a	(intercept)	-6.0912	< 0.0001	0.9147
		μ_{K_z}	-0.0193	< 0.0001	
		σ_{K_z}	0.0530	< 0.0001	
	M3a	(intercept)	-6.2570	< 0.0001	0.9227
		μ_{K_z}	-0.0193	< 0.0001	
		σ_{K_z}	0.0535	< 0.0001	
		M_U	0.00017	< 0.0001	
	M4a	(intercept)	-6.2600	< 0.0001	0.9227
		μ_{K_z}	-0.0193	< 0.0001	
		σ_{K_z}	0.0535	< 0.0001	
		M_U	0.00017	< 0.0001	
		S	0.00005	0.862	
	M5a	(intercept)	-6.2600	< 0.0001	0.9227
		μ_{K_z}	-0.0193	< 0.0001	
		σ_{K_z}	0.0535	< 0.0001	
		M_U	0.00017	< 0.0001	
		S	0.00005	0.862	
		SD	1.1110	0.904	
β_{max_b}	M1b	(intercept)	-3.3410	< 0.0001	0.9304
		μ_{K_z}	-0.0125	< 0.0001	
	M2b	(intercept)	-3.4610	< 0.0001	0.9341
		μ_{K_z}	-0.0125	< 0.0001	
		M_U	0.00013	< 0.0001	
	M3b	(intercept)	-3.4900	< 0.0001	0.9448
		μ_{K_z}	-0.0126	< 0.0001	
		M_U	0.00013	< 0.0001	
		σ_{K_z}	0.0025	< 0.0001	
	M4b	(intercept)	-3.4480	< 0.0001	0.9455
		μ_{K_z}	-0.0126	< 0.0001	
		M_U	0.00013	< 0.0001	
		σ_{K_z}	0.0024	< 0.0001	
		S	-0.00062	< 0.0001	
	M5b	(intercept)	-3.4480	< 0.0001	0.9455
		μ_{K_z}	-0.0126	< 0.0001	
		M_U	0.00013	< 0.0001	
		σ_{K_z}	0.0024	< 0.0001	
		S	-0.00062	< 0.0001	

		SD	0.2386	0.958	

Table 12: Summary of the main key drivers for the dependent variables $\boldsymbol{\beta_{SD\_b}}$ and $\boldsymbol{\beta_{max\_b}}$.

Dependent variables	**Independent variables**		**ΔR^2**	**Level of influence**
β_{SD_b}	μ_{K_z}	Support stiffness mean value	0.6506	30 to 100%
	σ_{K_z}	Support stiffness standard deviation	0.2641	10 to 30%
	M_U	Vehicle unsprung mass	0.0080	0 to 10%
	S	Travelling speed	0.0000	No influence
	SD	Irregularities standard deviation	0.0000	No influence
β_{max_b}	μ_{K_z}	Support stiffness mean value	0.9304	30 to 100%
	M_U	Vehicle unsprung mas	0.0037	0 to 10%
	σ_{K_z}	Support stiffness standard deviation	0.0107	0 to 10%
	S	Travelling speed	0.0007	0 to 10%
	SD	Irregularities standard deviation	0.0000	No influence

4.3. The influence of speed and axle load

The effect of speed and axle load is discussed further in this section, considering one support stiffness distribution and one vertical irregularity series (i.e. original data for site B).

Figure 11 and Figure 12 show the variation of β_{SD_b} and β_{max_b} respectively, for varying load and speed. They suggest that the speed is more crucial in localized corrective maintenance needs than in preventive maintenance needs. This is in line with previous results ([42]). The axle load, on the other hand, plays an important role and there is an increase of ca. 48.1% and 53.5% in case of β_{SD_b} and β_{max_b}, respectively, w.r.t. to the lowest load considered. These increments are hardly affected by the speed value, which can be explained with the choice of settlement law used in this study.

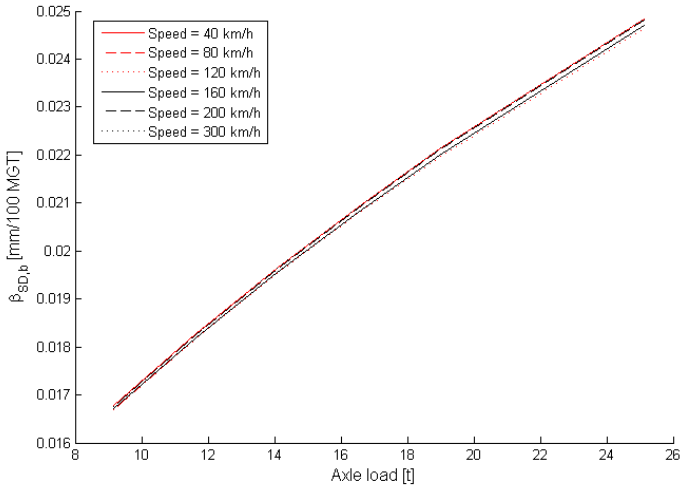

Figure 11: Variation of $\boldsymbol{\beta_{SD\_b}}$ for varying load and increasing speed.

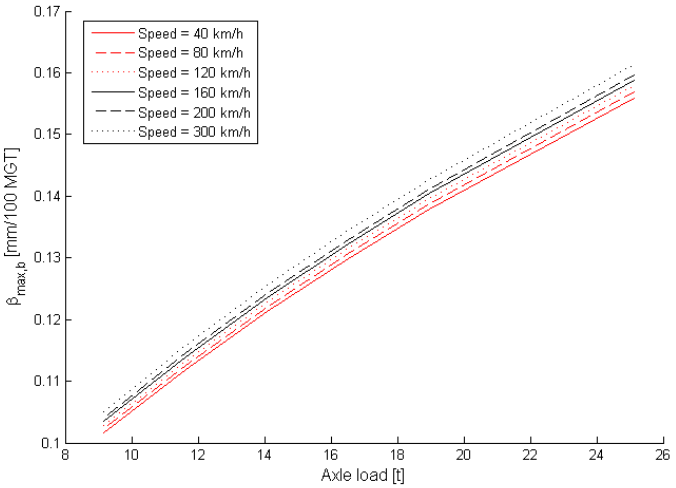

Figure 12: Variation of $\boldsymbol{\beta_{max\_b}}$ for varying load and increasing speed.

5. Conclusions and further work

The present work focused on characterising the role of vertical stiffness, both absolute and spatial variability, on the long-term deterioration of track quality. The data of support stiffness and vertical irregularity has been analysed using a sample procedure based on an ARIMA stochastic process. It has been demonstrated that the best fitting ARIMA model can take into account the naturally occurring longitudinal variation of the original data. Also, it has been shown that no model specification (p, d, q) can describe data regardless of the site. This might be because it is not possible to represent the localised characteristics in a general way. The property that a linear transformation of an ARIMA process is also an ARIMA process has been used to create a large number of new set of

data with given mean values and standard deviations. The same has been done to reproduce track irregularities inputs. It was also shown on the basis of the two given site data that both support stiffness and vertical irregularities series were not co-integrated and thus assumed in this work that they can be sampled independently from each other. Work on larger sets of data would be needed to confirm or not this observation.
Given these track geometry and support condition signals, a vertical vehicle-track interaction model has been used iteratively to calculate the evolution of the rail track irregularities under cumulative settlement action. A selection of parameters, including vehicle unsprung mass, vehicle speed, support stiffness characteristics (i.e. mean value and standard deviation) and rail irregularities standard deviation, has been varied to assess the influence of each parameters on the long-term behaviour of the track through a set of computational experiments.
Log-linear regression models were estimated and it was shown that the spatial variability of the vertical stiffness (i.e. standard deviation of vertical stiffness) has a statistically significant effect in the deterioration rates of vertical irregularities (either assessed locally by the maximum vertical defect or by the standard deviation). The main affecting parameters identified are the support stiffness characteristics and also to some extent, the vehicle unsprung mass for both the deterioration rate of the ballast settlement SD (β_{SD_b}) and the deterioration rate of the maximum ballast settlement (β_{max_b}). The speed only explains part of the variation in case of deterioration rate of the maximum ballast settlement. This suggests that speed have more influence on localised corrective maintenance needs than in preventive maintenance needs.
These findings contribute to focusing railway track design and construction on the quality control of support stiffness and, in particular, by limiting for instance the spatial variability of vertical stiffness in the track design process. It has to be noticed that these results also echo with challenges encountered with transitions zone and the control of stiffness variability and associated differential settlement. This is a topic of research the authors are involved in and for which the methodology presented here will be applied in future research.
Further research should also focus on the physical correlation between support stiffness and the track irregularities series. Another key area of research is identified in developing a suitable universal settlement equation based on combined physical testing and numerical modelling, which should better explain the influence of speed and loading frequency in particular.

Acknowledgements

This work has been funded by the Institute of Railway Research, the H2020 programme European project In2Rail (grant agreement n. 635900) and the UK EPSRC project Track to the Future (grant agreement n. EP/M025276/1).

References

1. Sussmann, T.R., W. Ebersohn, and E.T. Selig, *Fundamental nonlinear track load-deflection behavior for condition evaluation.* Transportation Research Record, 2001. **1742**: p. 61-67.

2. Hooke, R., *De Potentia Restitutiva, or of Spring Explaining the Power of Springing Bodies, vol. 1678.* London, UK: John Martyn: p. 23.

3. Berggren, E.G., A.M. Kaynia, and B. Dehlbom, *Identification of substructure properties of railway tracks by dynamic stiffness measurements and simulations.* Journal of Sound and Vibration, 2010. **329**: p. 3999-4016.

4. INNOTRACK, *Methods of track stiffness measureemnts*. 2006.

5. RIVAS, *D2.5: Overview of methods for measurement of track irregularities important for ground-borne vibration*. 2013.

6. Lopez Pita, A., P.F. Teixeira, and F. Robuste, *High speed and track deterioration: The role of vertical stiffness of the track.* Proceedings of the Institution of Mechanical Engineers, Part F: Journal of Rail and Rapid Transit, 2004. **218**: p. 31-40.

7. Li, M.X.D. and E.G. Berggren, *A study of the effect of global track stiffness and its variations on track performance: Simulation and measurements.* Proceedings of the Institution of Mechanical Engineers, Part F: Journal of Rail and Rapid Transit, 2010. **224**: p. 8.

8. Frohling, R.D., *Deterioration of railway track due to dynamic vehicle loading and spacially varying track stiffness* in *Faculty of Engineering*. 1997, University of Pretoria: Pretoria.

9. Dahlberg, T., *Railway track stiffness variations – consequences and countermeasures.* International Journal of Civil Engineering, 2010. **8**(1): p. 1-11.

10. Frohling, R.D., H. Scheffel, and W. Ebersohn, *The vertical dynamic response of a rail vehicle caused by track stiffness variations along the track.* Vehicle System Dynamics, 1996. **25 Suppl.1**: p. 13.

11. Dodge, Y., *Kolmogorov–Smirnov Test*, in *The concise encyclopedia of statistics*. 2008, Springer: New York. p. 283-287.

12. Cryer, J.D. and K.-S. Chan, *Time series analysis with applications in R*. 2 ed. 2008, New York: Springer-Verlag. 491.

13. Akaike, H., *Information theory and an extension of the maximum likelihood principle*, in *2nd International Symposium on Information Theory* B.N. Petrov and F. Csaki, Editors. 1973, Akadémia Kiado: Budapest. p. 267-281.

14. Hyndman, R., *Forecast Package v7.6: Forecasting Functions for Time Series and Linear Models*. 2016.

15. Fuller, W., *Introduction to Statistical Time Series*. 1976, New York: John Wiley & Sons, Inc.

16. Phillips, P.C. and P. Perron, *Testing for a unit root in time series regression.* Biometrika, 1988. **75**(2): p. 335-346.

17. Phillips, P.C. and S. Ouliaris, *Asymptotic properties of residual based tests for cointegration.* Econometrica: Journal of the Econometric Society, 1990: p. 165-193.

18. Grossoni, I., et al., *Dynamics of a vehicle–track coupling system at a rail joint.* Proceedings of the Institution of Mechanical Engineers, Part F: Journal of Rail and Rapid Transit, 2015. **229**(4): p. 364-374.

19. Zhai, W., K. Wang, and C. Cai, *Fundamentals of vehicle–track coupled dynamics.* Vehicle System Dynamics, 2009. **47**(11): p. 1349-1376.

20. Suiker, A.S.J. and R. de Borst, *A numerical model for the cyclic deterioration of railway tracks.* International Journal for Numerical Methods in Engineering, 2003. **57**(4): p. 441-470.

21. Dahlberg, T., *Some railroad settlement models—a critical review.* Proceedings of the Institution of Mechanical Engineers, Part F: Journal of Rail and Rapid Transit, 2001. **215**(4): p. 289-300.

22. Shenton, M. *Deformation of railway ballast under repeated loading conditions*. in *Symposium on Railroad Track Mechanics, RRIS 01 130826, Publication 7602*. 1975.

23. Selig, E.T. and J.M. Waters, *Track geotechnology and substructure management*. 1994: Thomas Telford.

24. Guerin, N., *Approche experimentale et numerique du comportement du ballast des voies ferrees*, in *Structures et materiaux*. 1996, Ecole nationale des ponts et chausses: Paris.

25. Stewart, H.E. and E. Selif, *Correlation of concrete tie track performance in revenue service and at the facility for accelerated service testing--volume ii: Predictions and evaluations of track settlement*. 1984.

26. Jeffs, T. and S. Marich. *Ballast characteristics in the laboratory*. in *Conference on Railway Engineering 1987: Preprints of Papers*. 1987. Institution of Engineers, Australia.

27. Indraratna, B. and W. Salim, *Deformation and degradation mechanics of recycled ballast stabilised with geosynthetics.* Soils and Foundations, 2003. **43**(4): p. 35-46.

28. Indraratna, B., N.T. Ngo, and C. Rujikiatkamjorn, *Deformation of coal fouled ballast stabilized with geogrid under cyclic load.* Journal of Geotechnical and Geoenvironmental Engineering, 2012. **139**(8): p. 1275-1289.

29. Indraratna, B. and S. Nimbalkar, *Stress-strain degradation response of railway ballast stabilized with geosynthetics.* Journal of geotechnical and geoenvironmental engineering, 2013. **139**(5): p. 684-700.

30. Thom, N. and J. Oakley. *Predicting differential settlement in a railway trackbed*. in *Proceedings of Railway foundations conference: Railfound*. 2006.

31. Cuellar, V., et al., *Short and long term behaviour of high speed lines as determined in 1:1 scale laboratory tests*, in *9th World Congress on Railway Research*. 2011: Lille.

32. Estaire, J. and F. Vincente, *CEDEX Track Box as an experimental tool to test railway tracks at 1:1 scale*, in *Proceedings of the 19th International Conference on Soil Mechanics and Geotechnical Engineering*. 2017: Seoul.

33. Abadi, T., et al., *A Review and Evaluation of Ballast Settlement Models using Results from the Southampton Railway Testing Facility (SRTF).* Procedia Engineering, 2016. **143**: p. 999-1006.

34. Partington, W., *TM-TS-097: Track deterioration study - Results of the track laboratory experiments*. 1979, British Railway Research: Derby.

35. Sato, Y., *Japanese studies on deterioration of ballasted track.* Vehicle System Dynamics, 1995. **24 Suppl.**(1): p. 197-208.

36. Frohling, R.D., *Low frequency dynamic vehicle-track interaction: modelling and simulation.* Vehicle System Dynamics, 1998. **29 Suppl.**(1): p. 30-46.

37. Hunt, G.A., *EUROBALT: vertical dynamic model for track damage studies*. 1996, British Rail Research.

38. Abadi, T., et al., *Improving the performance of railway tracks through ballast interventions.* Proceedings of the Institution of Mechanical Engineers, Part F: Journal of Rail and Rapid Transit, 2016. **232**(2): p. 337-355.

39. Basney, J., M. Livny, and T. Tannenbaum, *High throughput computing with Condor.* HPCU news, 1997. **1**(2): p. 1.

40. Steenbergen, M.J., *Physics of railroad degradation: The role of a varying dynamic stiffness and transition radiation processes.* Computers & Structures, 2013. **124**: p. 102-111.

41. Nielsen, J.C.O., et al., *Track geometry degradation on the Swedish heavy haul line – correlation between measured support stiffness gradients and differential settlement*, in *11th International Heavy Haul Conference*. 2017: Cape Town, South Africa.

42. Grossoni, I., A.R. Andrade, and Y. Bezin. *Assessing the role of longitudinal variability of vertical track stiffness in the long-term deterioration*. in *24th Symposium of the International Association for Vehicle System Dynamics*. 2015. Graz (Austria): CRC Press.